

Tunneling spectroscopy across GaAs/Al_xGa_{1-x}As interfaces at nanometer resolution

H. W. M. Salemink, O. Albrektsen,* and P. Koenraad†

IBM Research Division, Zurich Research Laboratory, CH-8803 Rüschlikon, Switzerland

(Received 22 October 1991)

The transition region at the interface of GaAs/Al_xGa_{1-x}As multilayers grown by molecular-beam epitaxy is investigated on the (110) face using scanning tunneling microscopy and spectroscopy. An interface region of 2 to 3 unit cells is observed in the charge-density contours. The tunneling spectroscopy data, on the other hand, yield a transition region of 6 to 9 unit cells wide, as determined from the offset of the valence-band edge. The experimentally derived valence-band position compares well with theoretical calculations, provided the tip-induced electrostatic band bending in the semiconductor layers is taken into account.

The electronic structure of semiconductor interfaces is of interest for fundamental and technological reasons. The adjustment of the electronic structure in heterojunctions is calculated theoretically from first principles;^{1,2} these calculations demonstrate that the electronic-charge density usually takes representative bulk values about two unit cells away from the heterointerface. Owing to the requirements for periodic boundary conditions in these numerical calculations, only ideal (averaged) crystal potentials and alloys are studied, excluding the effects of alloy disorder. The experimental determination of spatial variations of the electronic band structure at nanometer scales is important in order to analyze and predict electron-transport properties in heterostructures, particularly as these become smaller.³

Conventional experimental studies of the band structure (photoluminescence, electron transport, and photoemission) all involve a very large number of unit cells (10^3 – 10^5). In contrast, the scanning tunnel microscope (STM) allows atomic resolution to be combined with local spectroscopy on a (sub)nanometer scale^{4,5} on selected surfaces. We have exploited the STM technique to map the atomic charge density in (110) cross sections of GaAs/Al_xGa_{1-x}As multilayers grown by molecular beam epitaxy (MBE) and across their interfaces. Simultaneously with local current-voltage (I - V) spectroscopy, the electronic band structure at this (110) surface, in particular the valence-band edge, is acquired. Thus, the experiments combine atomic-resolution images with spectroscopy on a nanometer scale across synthetically grown multilayers.

The GaAs/Al_xGa_{1-x}As multilayers are MBE-grown along the preferential $\langle 001 \rangle$ direction; the results described in this paper pertain to nominal Al_x fractions of $x = 0.35$ – 0.38 in Al_xGa_{1-x}As. All structures are highly p -type doped with Be, typically 1×10^{19} cm⁻³ in GaAs and 6×10^{18} cm⁻³ in Al_xGa_{1-x}As: the different growth rates of the two materials account for the respective Be incorporation levels. The layered stack is cleaved in UHV (at a pressure of 1×10^{-10} mbar) to expose the (110) cross-sectional plane and is transferred into the STM unit, which operates at room temperature at a UHV pressure of $< 4 \times 10^{-11}$ mbar. A UHV-compatible

secondary-electron microscope is used to move the tunneling tip rapidly at the location of the semiconductor-multilayer stack with an accuracy of 25 nm.⁶ The GaAs (110) facet used in the experiments reported here is of interest for two reasons: first, the cross section is perpendicular to the growth direction and thus exposes the layers and their interfaces and, second, under clean conditions this facet is charge neutral with both Ga and As ions occupying surface sites. Moreover, since the surface states reside outside the fundamental band gap,⁷ the onset of the valence- and conduction-band edges can readily be observed with the local I - V tunneling spectra.⁸

On the clean GaAs (110) surface, we find the 1×1 unit-cell structure and the I - V spectra as reported previously.⁸ In the multilayer cross sections, we observe the atomic registry in the epitaxial GaAs and Al_xGa_{1-x}As layers as well as across their interface⁹ (Fig. 1). The material transition occurs over 1 to 2 unit cells (see arrows). The filled-state charge density is traced in these constant-current images and this quantity is closely connected with the local atomic potentials. Apparently, these properties change over the 1 to 2 unit-cell-length scale, in close agreement with theoretical predictions.^{1,2} We remark that in these binary/ternary compound interfaces no unique interfacial plane exists on the atomic scale.¹⁰ Apparent broadening of the interface due to convolution of the change in charge density with the tip wave function is considered to be small, since we detect atomic-scale fluctuations and the absence of individual atoms in the Al_xGa_{1-x}As material. The inhomogeneous charge density in the ternary material is attributed to the random composition fluctuations^{9,10} that become observable at atomic resolution. In the high-resolution TEM analysis which delivers a projected image, this alloy disorder is averaged out over multiple unit cells. Such alloy disorder is observed routinely in the Al_xGa_{1-x}As and In_xGa_{1-x}As_yP_{1-y} material investigated and will be the subject of further investigation.

Figure 1 displays an interface between Al_{0.38}Ga_{0.62}As and GaAs obtained with slightly lower spatial resolution compared with that in Ref. 9. A growth step approximately eight atoms high separating two (001) growth terraces is seen in the upper left part of this figure. The to-

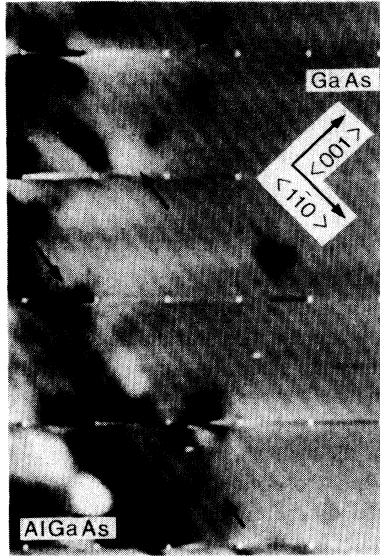


FIG. 1. Filled-state image on the (110) cross-sectional plane of the $\text{Al}_x\text{Ga}_{1-x}\text{As}/\text{GaAs}$ (inverted) interface. Sample voltage is -2.2 V. The white dots indicate the sampling positions of the current-voltage characteristics. Two growth terraces, separated by an eight-atom high step, are indicated by arrows. The $\langle 001 \rangle$ growth direction is indicated. Note the uniform appearance of the GaAs and the inhomogeneous charge density in $\text{Al}_x\text{Ga}_{1-x}\text{As}$.

pographic interface should be interpreted in the sense of the aforementioned composition fluctuations and thus is defined with an accuracy of ± 1 unit cell. The two $\{1\bar{1}0\}$ growth planes on this $\text{Al}_x\text{Ga}_{1-x}\text{As}/\text{GaAs}$ (inverted) interface are indicated by two sets of arrows.

Simultaneously with the acquisition of the topographic image in Fig. 1, current-voltage (I - V) curves were obtained at up to 64 positions per image; some of these positions are indicated by white dots in Fig. 1. The spatial separation in this grid is 3 unit cells or 1.7 nm. Representative sets of I - V characteristics across the heterointerface are reproduced in Fig. 2 (the curves are vertically offset for clarity); Figs. 2(a) and 2(b) are taken along a horizontal and vertical section, respectively. On the GaAs material these curves display a semiconductor band gap of approximately 1.5 eV free of electronic states and the onset of the valence and conduction band (VB and CB, respectively).^{8,9} For the highly p -type doped GaAs material, the Fermi level (E_F , $V_{\text{sample}}=0$) is close to the VB edge.⁹ The transition across the $\text{Al}_x\text{Ga}_{1-x}\text{As}$ is indicated by the drop of the observed VB-edge energy by approximately 0.30 eV. Empirically, it has proved difficult to acquire the highest-resolution topography simultaneously with stable spectroscopy curves on the (Al)GaAs (110) surfaces; in this experiment a tradeoff is made in favor of spectroscopy. We will henceforth concentrate quantitatively on the structure at the VB edge; the onset of the CB, specifically in the $\text{Al}_x\text{Ga}_{1-x}\text{As}$, is more complex and will be discussed elsewhere.

Various methods are used to determine the VB from the I - V curves; the most reliable are the comparisons with theoretically calculated curves.^{11,12} There are minor differences in the absolute values obtained, but the differential VB readings for the $\text{GaAs}/\text{Al}_x\text{Ga}_{1-x}\text{As}$ interfaces remain within the stated accuracy.

The VB-edge energy derived from nine spectroscopy sets like those in Fig. 2 is plotted in Fig. 3 as a function of relative distance across the interface; each I - V sampling position is adjusted to the topographic interface (zero at the x axis), to an accuracy of ± 2 unit cells. Thus, we obtain a plot of the VB-edge energy at the (110) plane across the interface in the $\langle 001 \rangle$ direction. The VB-edge values, experimentally found far from the interface (> 25 nm), are indicated (B). The dash line (C) is the calculated VB-edge position for the bulk material, taking the relevant doping levels into account. In order to explain the I - V curves and, specifically, the observed VB onset, we performed tunneling calculations for doped (Al)GaAs compounds, which include the vacuum barrier and the image-potential correction as well as the additional tunneling through the semiconductor band bending region.^{11,12} This latter band bending is dependent on the

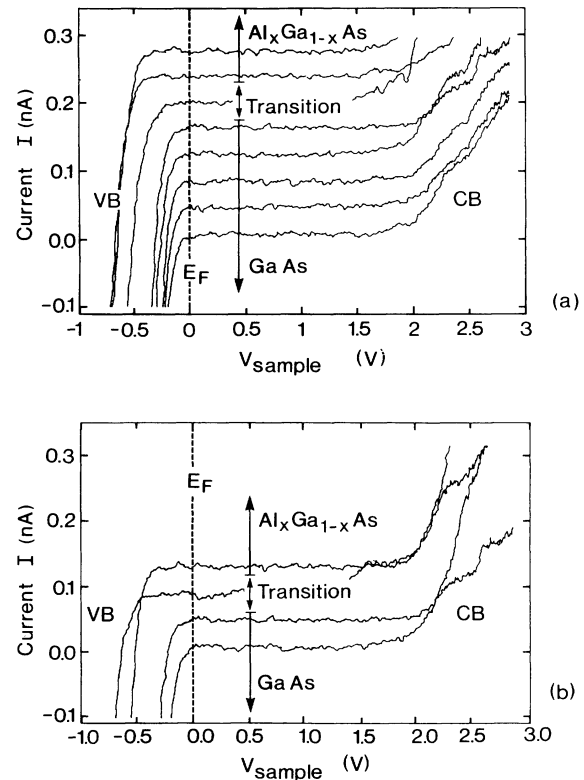


FIG. 2. (a) Set of current-voltage (I - V) characteristics taken across the $\text{Al}_x\text{Ga}_{1-x}\text{As}/\text{GaAs}$ interface of Fig. 1. Separation between sampling positions is 3 unit cells or 1.7 nm. The electronic interface is observed in the spectroscopy by the change in the valence-edge energy. The (I - V) spectra are taken along the horizontal axis. (b) Similar set of (I - V) spectra as in (a), taken along the vertical axis.

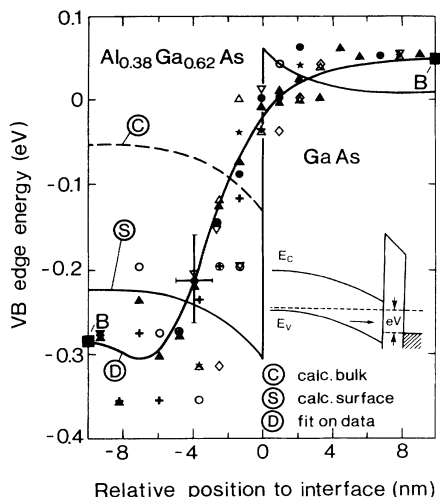


FIG. 3. Experimentally observed valence-band-edge energy across $\text{Al}_x\text{Ga}_{1-x}\text{As}/\text{GaAs}$ interface from multiple lines like those in Fig. 2. For comparison, the sampling positions are adjusted to the topographic interface as indicated in Fig. 2. The dashed line (C) represents the calculated position of the valence-band maximum for bulk material. The solid curve (S) displays the calculated position of the valence-band maximum for the tunneling spectroscopy at the (110) surface, taking the semiconductor depletion into account. The solid curve (D) displays a fit to the data. The inset shows the potential diagram for tunneling out of the valence band, including the vacuum barrier, tip-induced band bending, and the semiconductor depletion region.

actual doping level and forms an additional (solid-state) barrier for tunneling out of the bulk VB (see inset of Fig. 3). The expected VB-edge energy (S) is calculated for the tunnel spectroscopy on the (110) surface. For the actual doping level in the $\text{Al}_{0.38}\text{Ga}_{0.62}\text{As}$, the depletion barrier delays the current rise at the VB edge by about 0.15 eV and makes it observable at a corresponding lower energy, as indicated by the solid line in Fig. 3. Taking this additional tunneling process through the subsurface-depletion region into account, we find good agreement between the calculated S and experimentally observed D VB onsets in Fig. 3. The accuracy of the experiments and calculations is estimated at present to be ± 50 and ± 20 meV, respectively. A transition region for the VB edge of 3.5 to 5.0

nm (6 to 9 unit cells) has been determined; this value is close to the minimum length scale (λ_B) for a meaningful definition of a semiconductor valence-band maximum.¹⁰ The VB transition region is larger than the length scale calculated for the transition in the atomic potentials and charge density (1.0–1.5 nm), as computed for ideal interfaces,^{1,2} and wider than the transition region we observe in the charge density (Fig. 1 and Ref. 9). We believe that our results provide a good estimate for the extent of the electronic interface and the length scale at which the VB energy approximates a converged value. In the ternary $\text{Al}_x\text{Ga}_{1-x}\text{As}$ material, the statistical Al variations in the probing volume can account for part of the fluctuations we observe in the topography and spectroscopy. In the present experiments the limiting parameters are the compositional disorder on the atomic scale, the accuracy in aligning the spectroscopy curves to the material interface, the finite diameter of the tunneling filament (assumed to be $1 \times 1 \text{ nm}^2$), and the influence of the transverse \mathbf{k} vector. These effects will tend to broaden the interface width observed in the spectroscopy.

In addition, the imperfection of the inverted ternary/binary interface of Fig. 1 can be responsible for a graded valence-band transition. The main result in this work is the real-space observation of the change density at semiconductor interfaces occurring over 1 to 2 unit cells and an associated change in the valence-band-edge energy that extends over a slightly larger region of 3.5–5 nm.

The interface of MBE-grown $\text{GaAs}/\text{Al}_x\text{Ga}_{1-x}\text{As}$ layers on the (110) plane is investigated with atomic resolution in topography and simultaneously with local spectroscopy on a nanometer scale. In the charge density we observe a transition region of 1 to 2 unit cells across the interface; the electronic width of the interface, as deduced from the VB-edge offset, occurs over a length scale of 3.5–5.0 nm. This value is close to the minimum-length scale on which the VB definition becomes meaningful. Quantitatively we find good agreement between the VB maximum-energy position observed across the interface and tunneling calculations, provided the semiconductor depletion and the electrostatic, tip-induced band bending are taken into account.

We acknowledge the MBE growth of the structures by H. P. Meier and D. J. Arent and the assistance in processing by H. Richard. We are indebted to A. C. Warren and A. Baldareschi for their support in theoretical modeling. The discussions with P. Guéret are gratefully acknowledged.

*Also at Institute for Quantum Electronics, ETH Hönggerberg, CH-8093 Zürich, Switzerland; present address: Telecommunications Research Laboratory, DK-2970 Hørsholm, Denmark.

†Permanent address: Physics Department, Eindhoven University of Technology, NL-5600 MB Eindhoven, The Netherlands.

¹A. Baldareschi, S. Baroni, and R. Resta, *Phys. Rev. Lett.* **61**, 734 (1988).

²I. P. Batra, S. Ciraci, and A. Baratoff, in *Proceedings of the*

NATO Workshop on Condensed Systems and Low Dimensionality, Marmaris, Turkey, Vol. B 253 of *NATO Advanced Study Institute, Series B: Physics*, edited by J. C. Beeby (Plenum, New York, 1991), p. 557.

³*Band Structure Engineering in Semiconductor Microstructures*, Vol. 189 of *NATO Advanced Study Institute, Series B: Physics*, edited by R. A. Abram and M. Jaros (Plenum, New York, 1988).

- ⁴R. J. Hamers, R. M. Tromp, and J. E. Demuth, *Phys. Rev. Lett.* **56**, 1972 (1986).
- ⁵I. W. Lyo, E. Kaxiras, and Ph. Avouris, *Phys. Rev. Lett.* **63**, 1261 (1989); P. Bedrossian, R. D. Meade, K. Mortensen, D. M. Chen, J. A. Golovchenko, and D. Vanderbilt, *ibid.* **63**, 1257 (1989).
- ⁶O. Albrektsen and H. Salemink, *J. Vac. Sci. Technol. B* **9**, 779 (1991).
- ⁷J. R. Chelikowsky and M. L. Cohen, *Solid State Commun.* **29**, 267 (1979).
- ⁸R. M. Feenstra, J. A. Stroscio, J. Tersoff, and A. P. Fein, *Phys. Rev. Lett.* **58**, 1192 (1987).
- ⁹O. Albrektsen, D. J. Arent, H. P. Meier, and H. W. M. Salemink, *Appl. Phys. Lett.* **57**, 31 (1990).
- ¹⁰S. B. Ogale, A. Madhukar, F. Voillot, M. Thomsen, W. C. Tang, T.C. Lee, J. Y. Kim, and P. Chen, *Phys. Rev. B* **36**, 1662 (1987).
- ¹¹R. M. Feenstra and J. A. Stroscio, *J. Vac. Sci. Technol. B* **5**, 923 (1987).
- ¹²P. Koenraad, O. Albrektsen, and H. Salemink (unpublished).

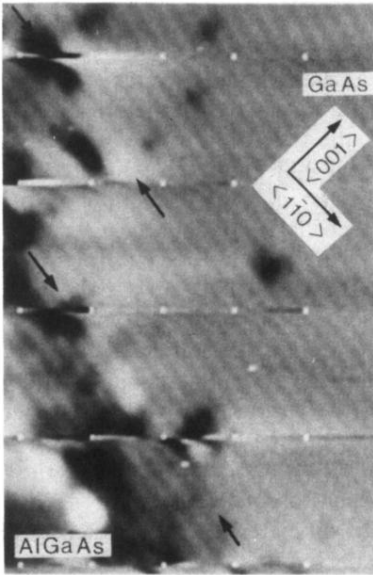


FIG. 1. Filled-state image on the (110) cross-sectional plane of the $\text{Al}_x\text{Ga}_{1-x}\text{As}/\text{GaAs}$ (inverted) interface. Sample voltage is -2.2 V. The white dots indicate the sampling positions of the current-voltage characteristics. Two growth terraces, separated by an eight-atom high step, are indicated by arrows. The $\langle 001 \rangle$ growth direction is indicated. Note the uniform appearance of the GaAs and the inhomogeneous charge density in $\text{Al}_x\text{Ga}_{1-x}\text{As}$.